MicroRNA-210 promotes angiogenesis in acute myocardial infarction

ZHONG-GUO FAN[1*], XIN-LIANG QU[1*], PENG CHU[1], YA-LI GAO[1], XIAO-FEI GAO[1,2], SHAO-LIANG CHEN[1,2] and NAI-LIANG TIAN[1,2]

[1]Department of Cardiology, Nanjing First Hospital, Nanjing Medical University; [2]Department of Cardiology, Nanjing Heart Center, Nanjing, Jiangsu 210006, P.R. China

Received March 5, 2017; Accepted November 14, 2017

DOI: 10.3892/mmr.2018.8620

Abstract. MicroRNA-210 (miRNA-210) has been reported to be associated with angiogenesis and may serve important roles in acute myocardial infarction (AMI), which remain unclear. The present study sought to evaluate the efficacy of miRNA-210 in AMI and to examine the potential associated mechanisms. AMI models were established in Sprague-Dawley rats. The expression of miRNA-210 was upregulated via transfection with lentivirus-mediated agonists and quantitative analysis was performed using the reverse transcription-quantitative polymerase chain reaction (RT-qPCR). Immunoblotting and RT-qPCR were separately used to detect the expression levels of hepatocyte growth factor (HGF) in heart samples, while only the protein expression level of β-myosin heavy chain (β-MHC) was assessed. The expression of HGF in human umbilical vein endothelial cells under hypoxic conditions was silenced by transfecting with small interfering RNA, as demonstrated by the determination of associated protein expression levels. The microvessel density (MVD) of the infarcted myocardium was selected to be the angiogenesis efficacy endpoint, which was evaluated by platelet endothelial cell adhesion molecule immunostaining. Markedly increased expression of HGF was observed among the AMI rats receiving miRNA-210 agonists, demonstrated via quantitative analyses using RT-qPCR or western blotting. Promotion of angiogenesis was observed with the increased MVD. Improved cardiac function in the rats was subsequently noted, as they exhibited improved left ventricular fractional shortening and left ventricular ejection fraction percentages, which may result from improved cardiac contractility indicated by attenuating the increase in β-MHC protein expression. Overexpression of miRNA-210 appeared to be an advantageous therapeutic tool for treating AMI, primarily due to its promoting effects on angiogenesis in the infarcted myocardium by stimulating HGF expression and inducing improved left ventricular remodeling, leading to improved cardiac function.

Correspondence to: Dr Nai-Liang Tian, Department of Cardiology, Nanjing First Hospital, Nanjing Medical University, 68 Changle Road, Nanjing, Jiangsu 210006, P.R. China
E-mail: tiannailiang@163.com

*Contributed equally

Key words: microRNA-210, acute myocardial infarction, hepatocyte growth factor, angiogenesis

Introduction

Ischemic heart disease is considered to be a leading cause of morbidity and mortality in humans, particularly those suffering from acute myocardial infarction (AMI). These patients are considered to be more susceptible to complications, including cardiogenic shock, or the development of chronic heart failure (CHF), although emergency revascularization has been widely used (1,2). It is likely that the loss of blood flow to the myocardium, primarily due to the occlusion of coronary arteries, may lead to myocardiocyte death and myocardial remodeling. As a result, improving myocardial recovery following AMI may exert positive effects in reducing the incidence of associated complications and leading to improved clinical outcomes.

MicroRNAs (miRNAs/miRs) are non-protein coding RNAs with a length of 22-24 nucleotides, which are able to interact with the 3'-untranslated regions of target mRNAs and inhibit transcription or translation (3). It has been previously reported that a number of miRNAs, including miRNA-34a, miRNA-208a and miRNA-495, may be important gene regulators for remodeling or inducing angiogenesis in response to AMI, and these beneficial effects have made non-coding RNAs potentially important therapeutic tools for preventing the appearance of CHF following AMI (4-6).

miRNA-210 serves an important role in response to hypoxic conditions and may be upregulated by hypoxia-inducing factors, and resultant alterations of cellular processes, including apoptosis, angiogenesis and metastasis, have been observed (7). Recently, Zeng *et al* (8) established ischemic brain models in mice and demonstrated that overexpression of miRNA-210 was able to enhance the microvessel density (MVD) in brain samples using immunohistochemistry analysis. Similar results were additionally reported by Yang *et al* (9), who demonstrated that miRNA-210 promoted hepatocellular carcinoma angiogenesis. In addition, Wang *et al* (10,11) reported different results pertaining to the effects of miRNA-210 in AMI,

although the same AMI rat models were used. It may be noted that the earlier formation of collateral circulation may reduce the risk of cardiomyocyte death and myocardial remodeling following AMI and facilitate improved clinical outcomes. However, these controversial data raised questions regarding the role of miRNA-210 in AMI. Therefore, the present study was designed to investigate the efficacy of miRNA-210 in AMI, and sought to elucidate the potential associated mechanisms.

Materials and methods

Animal experiments

Animals. A total of 48 Sprague-Dawley rats (4-week old; male) weighing 220-240 g were obtained from the Animal Center of Nanjing Medical University (Nanjing, China). All the rats were housed in the laboratory animal room maintained at a temperature of 20±2˚C with a relative humidity of 50-70% and on a regular 12 h light-dark cycle, with access to standard chow and water for 1 week prior to any operative procedures. The protocol of the animal experiments was approved by the Institutional Animal Care and Use Committee of Nanjing Medical University.

Rat model of AMI. The rats were anesthetized by intraperitoneal injection of 10% chloral hydrate (3 ml/kg) and a tracheotomy was subsequently performed, supported by a small animal ventilator (ALC-V8S; Shanghai Alcott Biotech Co., Ltd., Shanghai, China). The establishment of the AMI models was achieved by ligating the proximal left anterior descending (LAD) coronary artery with a 6-0 silk suture. A successful procedure was confirmed if the followed criteria were fulfilled: i) Observation of rapid discoloration over the anterior surface; and ii) electrocardiogram exhibiting persistent ST segment elevation ≥0.2 mV in two or more contiguous limb leads three times (reexamined every 10 min after the ligation). At the end of the surgery, all rats received an intramuscular injection of penicillin sodium (400,000 units) to prevent potential infection.

Animal groups and myocardial transfection with lentiviral vectors in vivo. The animals were randomly divided into 4 groups: i) Sham-operated (Sham; 12 rats) rats received all surgical procedures except for ligation of the LAD coronary artery; ii) AMI and treatment with negative control vector (AMI + NV; 7 rats); iii) AMI (AMI; 8 rats); and iv) AMI and treatment with lentivirus-mediated miRNA-210 agonist (AMI + LV-miR-210 agonist; 9 rats). The myocardial transfection *in vivo* was performed via intravenous injection with LV-miR-210 agonist (precursor-hsa-miR-210; Shanghai Genechem Co., Ltd., Shanghai, China) or negative control vector (hu6-MCS-Ubiquitin-EGFP-IRES-puromycin; Shanghai Genechem Co., Ltd.). The forward primer sequence for hsa-miR-210 was 5'-GGAAAGGACGAAACACCGGGGACAAGAGAGGAGTGGCTCTG-3', and the reverse primer sequence was 5'-TGTCTCGAGGTCGAGAATTAAAAAACTAGTGGCCCACTACCCTGTC-3', which were amplified into the 301-bp product as described previously (4). The negative control vector and LV-miRNA210 agonist were added to PBS to a final volume of 0.5 ml, which was applied to each rat, while untreated rats received PBS (0.5 ml) only.

Cardiac function assessment. A total of 4 weeks post-surgery, echocardiography using the Vevo2100 system (Fujifilm VisualSonics, Inc., Toronto, ON, Canada) with a high-frequency (30 MHz) MS-400 transducer was performed to evaluate the cardiac functions of the rats noninvasively. Prior to echocardiography, 3% isoflurane was used to induce anesthesia and maintenance with 1.5% isoflurane was applied during the procedure. The thickness of interventricular septum in systole and diastole, left ventricle internal dimension in systole (LVIDs) and diastole (LVIDd), thickness of LV posterior wall in systole (LVPWs) and diastole (LVPWd), left atrium (LA) internal dimension, LV volume in systole (LV VOLs) and diastole (LV VOLd), LV mass and LV mass corrected were measured. In addition, the LV fractional shortening percentage (FS) and LV ejection fraction percentage (EF) were calculated as followed: FS (%)=[(LVIDd−LVIDs)/LVIDd] x100; EF (%)=[(LV VOLd-LV VOLs)/LV VOLd] x100.

Preparation of tissue samples. Heart tissues were quickly removed from the sacrificed rats following the assessment of cardiac function. Each of the tissue samples was divided into two parts which were prepared for reverse transcription-quantitative polymerase chain reaction (RT-qPCR) analysis (temporarily stored at -80˚C) and immunohistochemical analysis (fixed in 4% paraformaldehyde at 20˚C, for 2 h) separately.

RT-qPCR analysis. In order to measure the expression levels of miRNA-210 and associated genes, heart samples were analyzed via RT-qPCR. Total RNA was extracted using TRIzol reagent (Zoonbio Biotechnology Co., Ltd., Nanjing, China) and transcribed into cDNA using the TransScript miRNA RT Enzyme Mix (TransGen Biotech Co., Ltd., Beijing, China; www.transbionovo.com/). The amplification of cDNA was subsequently performed following the protocol (95˚C for 30 sec, followed by 40 cycles at 95˚C for 5 sec, 60˚C for 20 sec) of the SYBR Premix Ex Taq II kit (Takara Biotechnology Co., Ltd., Dalian, China) using an ABI7500 system (Applied Biosystems; Thermo Fisher Scientific, Inc., Waltham, MA, USA). Human GAPDH was used as an internal control. The expression levels of miRNA-210, vascular endothelial growth factor (VEGF) and hepatocyte growth factor (HGF) were measured. The primer sequences of relative genes were as follows: GAPDH forward, 5'-GCAAGTTCAACGGCACAG-3' and reverse, 5'-GCCAGTAGACTCCACGACAT-3'; HGF forward, 5'-GGGGCTACACTGGATTGA-3' and reverse, 5'-GCCTTGATGGTGCTGACT-3'; miRNA-210 forward, 5'-AGCCACTGCCCACAGCACACTG-3' and reverse, 5'-CAGTGCAGGGTCCGAGGTATT-3'; and VEGF forward, 5'-CTCACCAAAGCCAGCACAT-3' and reverse, 5'-TTCTCCGCTCTGAACAAGG-3'. The comparative Cq method ($2^{-\Delta\Delta Cq}$) was used to analyze the data (12).

Immunohistochemistry. The paraffin-embedded heart samples were sliced into 4-5 μm thicknesses following dehydration, and were stained with hematoxylin-eosin (H&E; hematoxylin solution and 1% eosin solution, at room temperature for 10 min each) and prepared for Masson's trichrome staining (Bouin's solution, at 56˚C for 1 h at room temperature, Weigert hematoxylin working fluid for 20 min, then dying with ponceau red solution for 5 min, rinsing with distilled water for 30 sec, slides

were subsequently soaked in 1% phosphotungstic solution and dying with aniline blue solution, for 8 min each, at room temperature). MVD counting was performed on the basis of platelet endothelial cell adhesion molecule (CD31) immunohistochemistry. After deparaffinization [twice in xylene, 5 min each, followed by three sequential (90, 75 and 50%) solutions of ethanol, 5 min each], heart tissues were soaked in citrate buffer (0.01 mol/l, pH 6.0) to recover antigenicity. Subsequently, slides were incubated with 0.5% hydrogen peroxide-methanol solution for 10 min at room temperature. After rinsing with distilled water, rabbit anti-CD31 polyclonal antibody (1:100; cat. no. BA2966; Wuhan Boster Biological Technology, Ltd., Wuhan, China) was applied to sections as the primary antibody for 2 h at room temperature and the secondary antibody solution (1:500; cat. no. K5007; Dako; Agilent Technologies, Inc., Santa Clara, CA, USA) was added to induce horseradish peroxidase binding, maintained at room temperature for 30 min, following the methods described by Mineo *et al* (13). For each sample, at least 2 fields were selected for analysis. All the images were obtained using a light microscope (magnification, x200; Nikon Corporation, Tokyo, Japan), among which three areas with highest MVD in each section were selected for counting and the average of these vascular counts (mean intensity=integral optical density sum/area) was recorded as the MVD level in each case, quantified using image analysis software (Image Pro Plus 6.0; Media Cybernetics, Inc., Rockville, MD, USA).

Cell experiments

Cell culture and regent exposure. Human umbilical vein endothelial cells (HUVECs) cultured in Dulbecco's modified Eagle's medium (Gibco; Thermo Fisher Scientific, Inc.) were obtained from the American Type Culture Collection (Manassas, VA, USA). Cells cultured under normal oxygen levels were maintained at 37˚C and supplemented with 10% fetal bovine serum (Gibco; Thermo Fisher Scientific, Inc.) in a humidified chamber with 5% CO_2 and 95% air (labeled as the normoxia condition). The fresh culture medium was changed every day. Simultaneously, parallel cultured cells under hypoxic conditions were cultured as previously described (14).

Small interfering RNA (siRNA) transfection. The cells cultured under hypoxic condition were divided into two groups when they reached 50% confluence and were transfected with specific siRNA (The sequences were as follows: Upstream primer, GCUACAAGAAACCGCCUAUTT; downstream primer, AUAGGCGGUUUCUUGUAGCTT) for silencing HGF expression (100 nM/1.5x10^5 cells; labeled siHGF) or scrambled probe, as the negative control (both Sigma-Aldrich; Merck KGaA, Darmstadt, Germany). Lipofectamine RNAiMax (Invitrogen; Thermo Fisher Scientific, Inc.) was used, according to the manufacturer's protocol. Following 48 h of incubation, further western blot analyses were performed to evaluate the transfection efficiency and detect alterations in CD31 protein expression levels in these cells.

Western blot analysis. Each of heart samples was homogenized in lysis buffer with protease inhibitors (p0013c; Beyotime Institute of Biotechnology, Haimen, China) and centrifuged at 16,200 x g for 15 min at a temperature of 4˚C. To determine the protein concentration, the Pierce Bicinchoninic Acid protein assay (Thermo Fisher Scientific, Inc.) was used. Extracted protein samples were separated using 8-15% SDS-PAGE and subsequently transferred to polyvinylidene difluoride membranes (40 μg protein/lane). The membranes were blocked with 5% skimmed milk in TBS for 1 h at 37˚C. Rabbit polyclonal antibodies against HGF (1:400; cat. no. BA0911; Wuhan Boster Biological Technology, Ltd.) and β-myosin heavy chain (MHC) (1:500; cat. no. ab50967; Abcam, Cambridge, UK) were diluted with blocking buffer, in which the membranes were maintained overnight at 4˚C and washed with TBS-Tween-20 four times for 5 min each the following day. The membranes were subsequently incubated in blocking buffer with added secondary antibodies (1:5,000; cat. no. ABP103; Zoonbio Biotechnology Co., Ltd.) for 2 h at room temperature. Rabbit anti-rat β-actin (1:2000; cat. no. 8457; Cell Signaling Technology, Inc., USA) was applied as an internal control.

Following 48 h of incubation, transfected cells were lysed with radioimmunoprecipitation buffer (p0013c; Beyotime Institute of Biotechnology) containing protease and phosphatase inhibitors, and centrifuged at 13,800 x g for 20 min at 4˚C. The remainder of the protocol was as described above. However, the protein expression levels of HGF and CD31 (1:1,000; cat. no. 77699; Cell Signaling Technology, Inc., Danvers, MA, USA) were detected in the cells and GAPDH (1:1,000; cat. no. 5174; Cell Signaling Technology, Inc.) was used as the internal control. The Syngene Bio Imaging Device (Syngene Europe, Cambridge, UK) was used to visualize immunoreactive protein bands.

Statistical analysis. Statistical analysis was performed using the SPSS 22.0 software package (IBM Corp., Armonk, NY, USA) and all data are expressed as the mean ± standard deviation. One-way analysis of variance followed by Bonferroni corrections was used for comparisons between multiple groups. $P<0.05$ (two-tailed) was considered to indicate a statistically significant difference.

Results

AMI increases myocardial miRNA-210 expression. As depicted in Fig. 1A, myocardial miRNA-210 expression was increased significantly in the AMI + PBS subgroup compared with the sham group ($P=0.011$) at 4 weeks post-surgery. The expression level of miRNA-210 in the AMI + miR-210 agonist group was additionally significantly increased, compared with the other three subgroups ($P<0.001$ vs. Sham + PBS, AMI + NV and AMI + PBS, respectively). Notably, the comparison between the AMI + PBS group and AMI + NV group demonstrated a significant decrease in miRNA-210 expression in the latter group ($P=0.038$) and no statistical difference between the Sham + PBS group and the AMI + NV group was observed ($P=0.799$).

Overexpression of miRNA-210 up-regulates HGF expression. An apparent upregulation of HGF was observed in the AMI + miR-210 agonist subgroup compared with the other three subsets ($P=0.02$ vs. Sham + PBS; $P=0.049$ vs. AMI + NV; $P=0.048$ vs. AMI + PBS; Fig. 1B), which was principally driven by the overexpression of miRNA-210. However, the

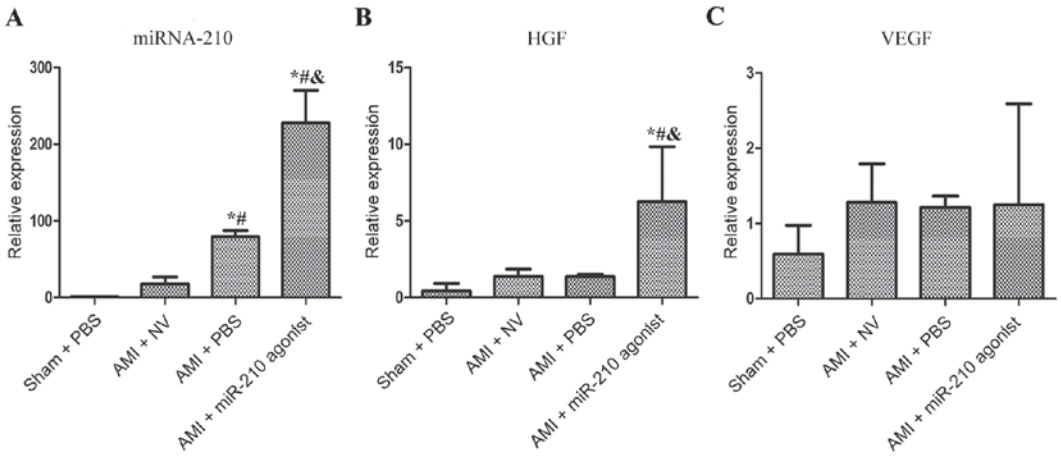

Figure 1. Relative expression levels of miRNA-210, HGF and VEGF in the rat myocardium at 4 weeks post-surgery, based on quantitative analysis. (A) The relative expression level of miRNA-210 in heart samples from each of the four subgroups. (B) The relative expression level of HGF in heart samples. (C) The relative expression level of VEGF in heart samples. All the analyzed data are expressed as the mean ± standard deviation. *P<0.05 vs. Sham + PBS; #P<0.05 vs. AMI + NV; &P<0.05 vs. AMI + PBS. n=3/group. miRNA/miR, microRNA; HGF, hepatocyte growth factor; VEGF, vascular endothelial growth factor; NV, negative control vector; AMI, acute myocardial infarction.

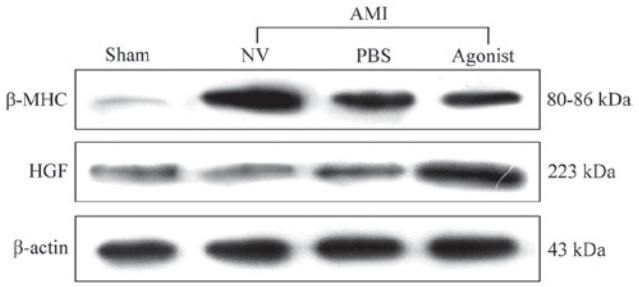

Figure 2. Representative western blot analysis of HGF and β-MHC protein expression in the rat myocardium at 4 weeks post-surgery. AMI, acute myocardial infarction; β-MHC, β-myosin heavy chain; HGF, hepatocyte growth factor; NV, negative control vector.

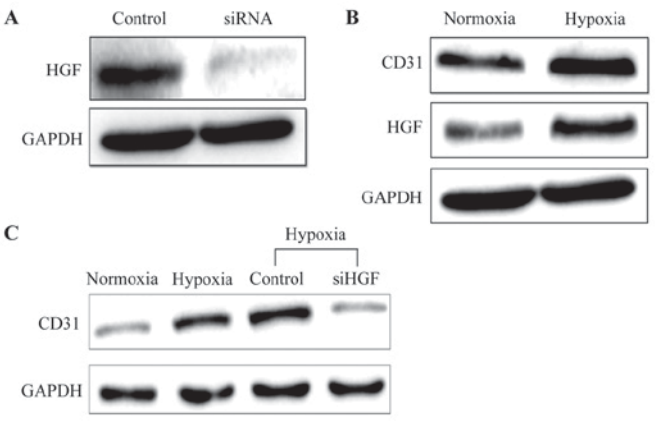

Figure 3. Protein expression levels of HGF and CD31 in HUVECs exposed to different conditions. (A) The suppressive effect of siRNA on HGF expression was determined by western blotting. (B) Representative western blot analysis of HGF and CD31 protein expression in cells exposed to normoxic or hypoxic conditions. (C) The protein expression levels of CD31 in HUVECs when treated with HGF siRNA or negative controls, following exposure to normoxic or hypoxic conditions. HGF, hepatocyte growth factor; CD31, platelet endothelial cell adhesion molecule; si, small interfering; HUVEC, human umbilical vein endothelial cell.

AMI-induced overexpression of miRNA-210 did not promote myocardial HGF expression (P=0.921 vs. Sham group) and the comparisons between multiple groups demonstrated no significant differences in the expression of VEGF (Fig. 1C). In addition, similar results in terms of protein expression levels exhibited an upregulation of HGF associated with miRNA-210 overexpression (Fig. 2). The attenuating increase of myocardial β-MHC protein expression induced by AMI was observed following treatment with miR-210 agonists, particularly compared with the AMI + NV group. These findings indicated that HGF may be a target gene of miRNA-210 in AMI.

Role of HGF in HUVEC proliferation. As presented in Fig. 3A, the protein expression level of HGF in HUVECs was decreased markedly following transfection with siRNA, demonstrating the suppressive effect of siRNA on HGF expression. Additionally, simultaneously increased CD31 and HGF protein expression was observed in the cells under hypoxic condition (Fig. 3B). When the HGF expression was silenced through transfection with siRNA, the level of CD31 protein expression in cells under hypoxic conditions was decreased, as depicted in Fig. 3C, indicating that HGF may be an important stimulator of HUVEC growth and proliferation.

Alterations induced by overexpression of miRNA-210 in histology and cardiac function

MVD in heart samples. MVD was measured in myocardial samples (Fig. 4). Compared with the sham group (Fig. 4A), a markedly decreased optical intensity of CD31 cells was noted in the myocardium in the AMI + NV subgroup (P=0.045; Fig. 4B and E). By contrast, the optical intensity of CD31 cells in the infarcted area of the heart treated with the miR-210 agonist was significantly increased compared with the AMI + NV group (P=0.029; Fig. 4D and E), whereas no statistical significance was observed when compared with the Sham group (P=0.996). The comparison between the AMI + NV group and AMI + PBS group indicated no significant difference (P=0.716; Fig. 4C and E). Therefore, better promoting angiogenesis effects with respect to over expression of miRNA-210 were observed.

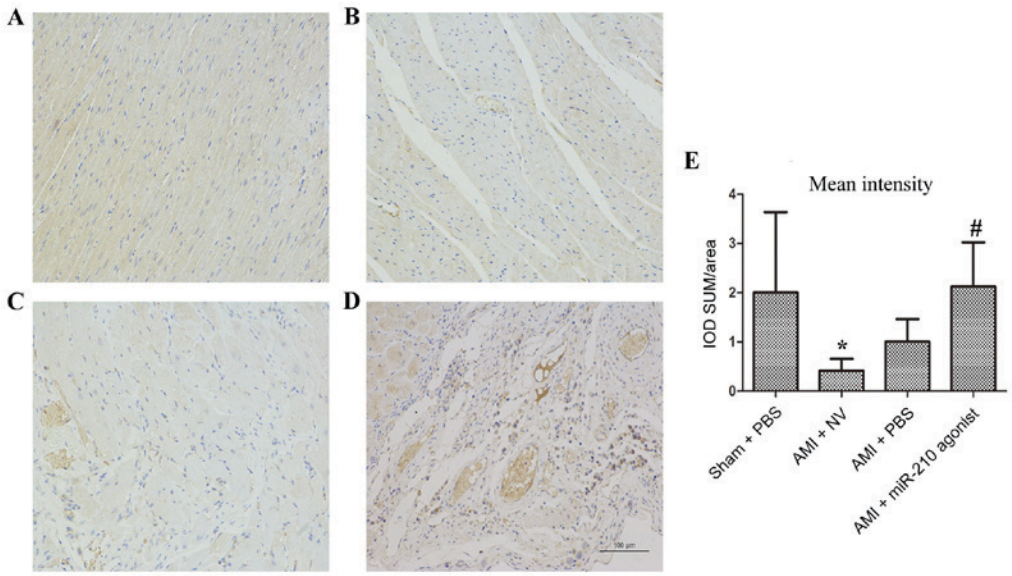

Figure 4. CD31 immunohistochemistry detects the presence of microvessels in the rat myocardium and the MVD levels of different groups. (A) Sham group. (B) AMI + NV group. (C) AMI + PBS group. (D) AMI + miR-210 agonist group. (E) Quantitative analysis of MVD levels. MVD counts in each case were expressed using the following formula: mean intensity=IOD SUM/area, and the comparisons between multiple groups were based on mean values. *P<0.05 vs. Sham + PBS; #P<0.05 vs. AMI + NV. n=3/group. CD31, platelet endothelial cell adhesion molecule; AMI, acute myocardial infarction; miR, microRNA; NV, negative control vector; IOD SUM, integral optical density sum; MVD, microvessel density.

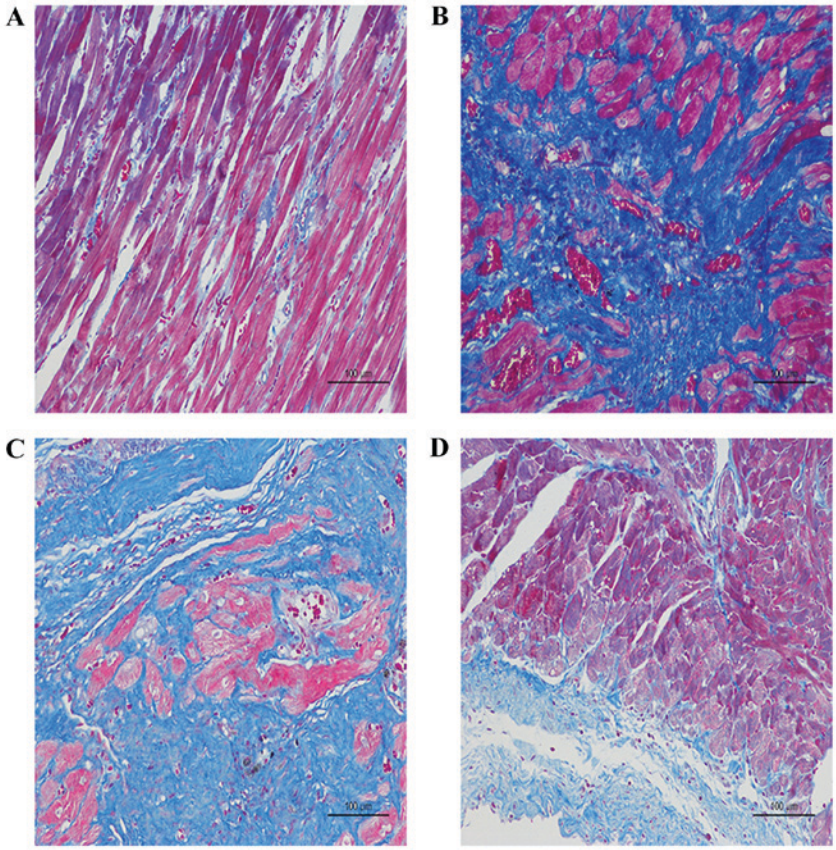

Figure 5. Histopathological observations of rat heart tissues in different subgroups under the light microscope. (A) Sham group. (B) AMI + NV group. (C) AMI + PBS group. (D) AMI + microRNA-210 agonist group. AMI, acute myocardial infarction; NV, negative control vector.

Histopathological observation of rat heart tissue. As presented in the images of H-E and Masson's trichrome staining, the diffuse, edematous myocardial fibers were severely broken, taking the form of deranged cellular structures among which a large number of collagen fibers had been accumulated in the AMI + NV group and the AMI + PBS group, compared with the Sham group (Fig. 5A-C). Improved results were observed with miRNA-210 agonists, indicating reduced accumulation

Table I. Alterations in cardiac structure and function at 4 weeks post-surgery.

	Group			
Parameter	Sham + PBS (n=12)	AMI + NV (n=7)	AMI + PBS (n=8)	AMI + LV miR-210 agonist (n=9)
IVSs, mm	2.56±0.35	1.97±0.41	2.91±0.15	3.08±0.52[b]
IVSd, mm	1.61±0.13	1.47±0.38	1.80±0.17	1.84±0.27
LVIDs, mm	3.76±0.77	6.64±0.46[a]	5.24±0.65	4.39±0.90[b]
LVIDd, mm	6.40±1.18	8.76±1.19	8.02±0.62	7.44±0.81
LA, mm	3.72±0.80	4.98±0.80	4.14±0.15	4.20±0.65
LVPWs, mm	2.93±0.18	2.68±0.33	2.77±0.20	2.98±0.37
LVPWd, mm	1.90±0.18	1.93±0.16	1.97±0.09	2.01±0.15
LV Mass, mg	751.03±175.18	1202.90±332.57	1180.24±84.26	1073.77±75.05
LV Mass Cor, mg	600.82±140.14	962.32±266.05	944.20±67.41	859.02±60.05
LV VOLs, μl	69.92±31.48	227.71±35.30[a]	133.61±37.85	91.07±45.20[b]
LV VOLd, μl	215.07±90.12	428.11±131.76	348.11±61.50	295.68±70.30
EF, %	71.15±3.46	45.22±8.43[a]	61.90±6.52[b]	67.26±5.84[b]
FS, %	41.37±2.87	23.73±5.51[a]	34.76±4.90	38.45±4.16[b]

[a]P<0.05 vs. Sham + PBS; [b]P<0.05 vs. AMI + NV. s, systole; d, diastole; IVS, thickness of interventricular septum; LVID, left ventricular internal dimension; LA, left atrium; LVPW, thickness of left ventricular posterior wall; LV Mass, mass of left ventricle; Cor, corrected; LV VOL, left ventricular volume; EF, ejection fraction; FS, fractional shortening.

of collagen fibers and decreased destruction of myocardial fibers (Fig. 5D).

Cardiac function changes. Echocardiography was performed on the rats to evaluate alterations in cardiac structure and function at 4 weeks post-surgery. Compared with the Sham group, the cardiac contractility was markedly decreased in the AMI + NV group, which was primarily derived from the enlarged LVD and LV VOL in systole, resulting in a decrease in LVEF and LVFS. By contrast, the hearts receiving the miRNA-210 agonist exhibited improved cardiac contractility compared with the AMI + NV groups at the same points, and improved results in LVEF and LVFS were acquired, while no significant difference compared with the Sham group was observed. The characteristics of alterations in cardiac structure and function among the rats are summarized in Fig. 6 and Table I.

Discussion

The resulting myocardiocyte death and myocardial remodeling post-AMI, derived from the occlusion of associated coronary arteries which may completely block blood flow to the myocardium, has been hypothesized to be the most important risk factor for the development of heart failure among these patients (2). Therefore, reperfusion therapy strategies have been widely applied in the clinic and demonstrated to be beneficial, regardless of emergency revascularization or thrombolytic therapy (15). The concept of using gene therapy to stimulate the regenerative abilities of the body for damaged tissues had been proposed as a potential therapeutic strategy for AMI. A number of miRNAs have been reported to act as potential therapeutic tools, primarily as regulators of target gene expression inducing

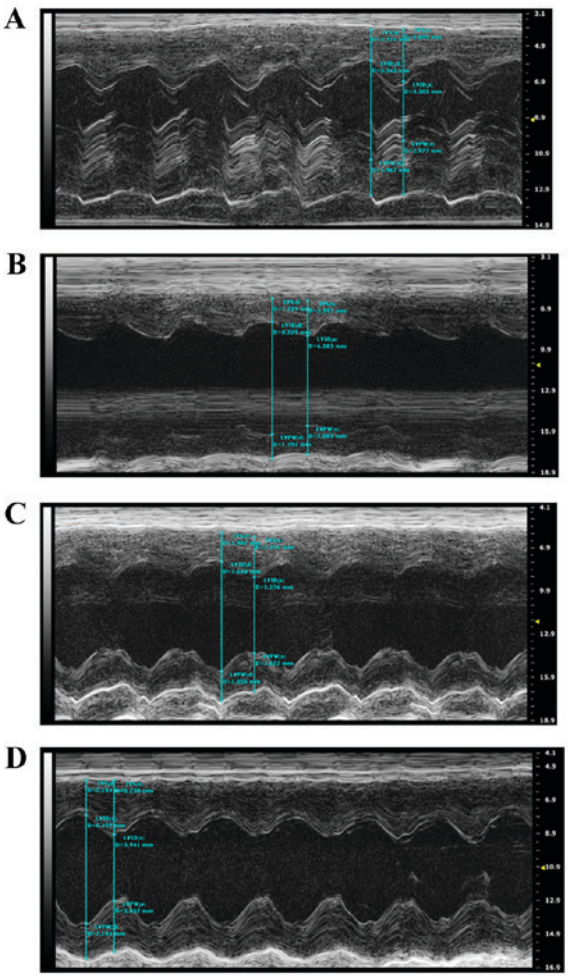

Figure 6. Doppler echocardiographic images obtained from the hearts of rats from different groups. (A) Sham group. (B) AMI + NV group. (C) AMI + PBS group. (D) AMI + microRNA-210 agonist group. AMI, acute myocardial infarction; NV, negative control vector.

therapeutic angiogenesis or attenuating remodeling in response to ischemic states (4-6,14,16). miRNA-210 serves a role in response to hypoxic conditions, and has been observed to be an important regulator in angiogenesis. Wang *et al* (10) reported that the knockdown of miRNA-210 expression led to improved cardiac function in AMI, while the opposite results were described by Wang *et al* (11), in which protective effects of the upregulation of miRNA-210 and VEGF were observed in AMI, which were hypothesized to be derived from the promotion of myocardial angiogenesis. These controversial data, in addition to the unclear mechanisms, called the role of miRNA-210 in AMI into question. As a result, the present study was performed and the principal finding was that overexpression of miRNA-210 induced by agonists exerted positive effects on promoting angiogenesis in AMI through the potential mechanism of upregulating HGF expression, which may serve a role in reducing remodeling following AMI and lead to better clinical outcomes in terms of improved cardiac contractility.

HGF, similar to VEGF, has been demonstrated to be an important stimulator of angiogenesis, exerting promotive effects on endothelial cell (EC) growth, proliferation, migration and differentiation (17-19). Gorin *et al* (17) demonstrated that HGF was exhibited a high angiogenic potential due to the direct targeting of ECs, and the results of the present study were consistent with these findings. Among the rats receiving miRNA-210 agonists in the present study, the upregulation of HGF induced by miRNA-210 overexpression exhibited promotive effects on angiogenesis in *in vivo* and *in vitro* experiments, as confirmed by CD31 immunohistochemistry. In addition, the increased proliferation and migration of ECs associated with HGF expression was indicated by Kaga *et al* (18). The underlying mechanism was reported to be associated with enhanced intracellular signaling molecules, including focal adhesion kinase and RAC-α serine/threonine-protein kinase, with respect to the regulation of cytoskeletal remodeling, cellular migration and morphogenesis (20). The results of the present study indicated that angiogenesis in AMI was induced by miRNA-210 overexpression via direct targeting of HGF, instead of VEGF, which was different from the observations of certain previous studies (10,11). The balance between proliferation and migration in ECs and vascular smooth muscle cells (VSMCs) may be considered to serve an important role in angiogenesis. Basic fibroblast growth factor (bFGF) has been reported to upregulate aquaporin 1 mRNA expression in HUVECs, thereby influencing vascular permeability (21). However, bFGF promoted the production of inflammatory factors, including C-C motif chemokine 2 and interleukin-8, as the activation of nuclear factor-κB and the number of VSMCs was additionally increased, whereas HGF and VEGF did not (18). HGF has been suggested to be an anti-inflammatory gene, due to its antioxidant effect in VSMCs (22,23). To the best of our knowledge, the acute phase of AMI is frequently complicated by a severe inflammatory response, leading to negative effects on the proliferation and migration of ECs; this may explain the results indicated in the present study, as the anti-inflammatory effect of HGF appeared to facilitate the balance between proliferation and migration in ECs and VSMCs, and subsequently to promote angiogenesis in AMI.

In order to examine the potential mechanisms of miRNA-208a with respect to myocardial remodeling post-AMI, Shyu *et al* (4) performed experiments *in vivo* and *in vitro*, and demonstrated that miRNA-208a served an important role in the development of myocardial fibrosis following AMI, primarily through its regulatory effects on endoglin expression, in addition to potent targeting effects on β-MHC. In the present study, improved cardiac functions were observed on the basis of improved cardiac contractility among the rats receiving miRNA-210 agonists, as demonstrated by echocardiography and western blot analysis of β-MHC. Left ventricular remodeling post-AMI may lead to a temporary compensatory enhancement of left ventricular systolic function, indicating a marked increase in β-MHC protein expression, which may increase myocardial oxygen demand and result in worse clinical outcomes. The results of the present study illustrated the attenuating increase of β-MHC protein expression, and were consistent with the results described by Wang *et al* (24); therefore, this may be an effective interpretation of the antifibrotic effect associated with microvascular formation induced by miRNA-210 overexpression, which was primarily due to the improved blood flow following maturation of new blood vessels, forming complete collateral circulation to increase the supply of oxygenated blood to myocardial cells.

In conclusion, the present study provided evidence to support the protective effects of overexpression of miRNA-210 in AMI, which were considered to be due to the promotion of angiogenesis in the infarcted myocardium by targeting HGF expression and inducing improved left ventricular remodeling post-AMI. Therefore, the overexpression of miRNA-210 may be suggested to be an advantageous therapeutic tool for treating AMI in order to obtain improved clinical outcomes.

Acknowledgements

The present study was supported by the Jiangsu Provincial Special Program of Medical Science (grant no. BL2013001).

References

1. Goldberg RJ, Spencer FA, Gore JM, Lessard D and Yarzebski J: Thirty-year trends (1975 to 2005) in the magnitude of, management of, and hospital death rates associated with cardiogenic shock in patients with acut: A population-based perspective. Circulation 119: 1211-1219, 2009.
2. McManus DD, Chinali M, Saczynski JS, Gore JM, Yarzebski J, Spencer FA, Lessard D and Goldberg RJ: 30-year trends in heart failure in patients hospitalized with acute myocardial infarction. Am J Cardiol 107: 353-359, 2011.
3. Bartel DP: MicroRNAs: Genomics, biogenesis, mechanism, and function. Cell 116: 281-297, 2004.
4. Shyu KG, Wang BW, Cheng WP and Lo HM: MicroRNA-208a increases myocardial endoglin expression and myocardial fibrosis in acute myocardial infarction. Can J Cardiol 31: 679-690, 2015.
5. Yang Y, Cheng HW, Qiu Y, Dupee D, Noonan M, Lin YD, Fisch S, Unno K, Sereti KI and Liao R: MicroRNA-34a plays a key role in cardiac repair and regeneration following myocardial infarction. Circ Res 117: 450-459, 2015.
6. Liang J, Huang W, Cai W, Wang L, Guo L, Paul C, Yu XY and Wang Y: Inhibition of microRNA-495 enhances therapeutic angiogenesis of human induced pluripotent stem cells. Stem Cells 35: 337-350, 2017.
7. Dang K and Myers KA: The role of hypoxia-induced miR-210 in cancer progression. Int J Mol Sci 16: 6353-6372, 2015.

8. Zeng LL, He XS, Liu JR, Zheng CB, Wang YT and Yang GY: Lentivirus-mediated overexpression of MicroRNA-210 improves long-term outcomes after focal cerebral ischemia in mice. CNS Neurosci Ther 22: 961-969, 2016.
9. Yang Y, Zhang J, Xia T, Li G, Tian T, Wang M, Wang R, Zhao L, Yang Y, Lan K and Zhou W: MicroRNA-210 promotes cancer angiogenesis by targeting fibroblast growth factor receptor-like 1 in hepatocellular carcinoma. Oncol Rep 36: 2553-2562, 2016.
10. Wang Y, Pan X, Fan Y, Hu X, Liu X, Xiang M and Wang J: Dysregulated expression of microRNAs and mRNAs in myocardial infarction. Am J Transl Res 7: 2291-2304, 2015.
11. Wang J, Zhang Y, Liu YM, Guo LL, Wu P, Dong Y and Wu GJ: Huoxue Anxin Recipe (HAR) promotes myocardium angiogenesis of acute myocardial infarction rats by up-regulating miR-210 and vascular endothelial growth factor. Chin J Integr Med 22: 685-690, 2016.
12. Livak KJ and Schmittgen TD: Analysis of relative gene expression data using real-time quantitative PCR and the 2(-Delta Delta C(T)) method. Methods 25: 402-408, 2001.
13. Mineo TC, Ambrogi V, Baldi A, Rabitti C, Bollero P, Vincenzi B and Tonini G: Prognostic impact of VEGF, CD31, CD34, and CD105 expression and tumour vessel invasion after radical surgery for IB-IIA non-small cell lung cancer. J Clin Pathol 57: 591-597, 2004.
14. Ye P, Liu J, He F, Xu W and Yao K: Hypoxia-induced deregulation of miR-126 and its regulative effect on VEGF and MMP-9 expression. Int J Med Sci 11: 17-23, 2013.
15. Levine GN, Bates ER, Blankenship JC, Bailey SR, Bittl JA, Cercek B, Chambers CE, Ellis SG, Guyton RA, Hollenberg SM, *et al*: 2015 ACC/AHA/SCAI focused update on primary percutaneous coronary intervention for patients with ST-elevation myocardial infarction: An update of the 2011 ACCF/AHA/SCAI guideline for percutaneous coronary intervention and the 2013 ACCF/AHA guideline for the management of ST-elevatio myocardial infarction. J Am Coll Cardiol 67: 1235-1250, 2016.
16. Li Q, Yu P, Zeng Q, Luo B, Cai S, Hui K, Yu G, Zhu C, Chen X, Duan M and Sun X: Neuroprotective effect of hydrogen-rich saline in global cerebral ischemia/reperfusion rats: Up-regulated tregs and down-regulated miR-21, miR-210 and NF-κB expression. Neurochem Res 41: 2655-2665, 2016.
17. Gorin C, Rochefort GY, Bascetin R, Ying H, Lesieur J, Sadoine J, Beckouche N, Berndt S, Novais A, Lesage M, *et al*: Priming dental pulp stem cells with fibroblast growth factor-2 increases angiogenesis of implanted tissue-engineered constructs through hepatocyte growth factor and vascular endothelial growth factor secretion. Stem Cells Transl Med 5: 392-404, 2016.
18. Kaga T, Kawano H, Sakaguchi M, Nakazawa T, Taniyama Y and Morishita R: Hepatocyte growth factor stimulated angiogenesis without inflammation: Differential actions between hepatocyte growth factor, vascular endothelial growth factor and basic fibroblast growth factor. Vascul Pharmacol 57: 3-9, 2012.
19. Awada HK, Johnson NR and Wang Y: Dual delivery of vascular endothelial growth factor and hepatocyte growth factor coacervate displays strong angiogenic effects. Macromol Biosci 14: 679-686, 2014.
20. Sulpice E, Ding S, Muscatelli-Groux B, Bergé M, Han ZC, Plouet J, Tobelem G and Merkulova-Rainon T: Cross-talk between the VEGF-A and HGF signalling pathways in endothelial cells. Biol Cell 101: 525-539, 2009.
21. Saadoun S, Papadopoulos MC, Hara-Chikuma M and Verkman AS: Impairment of angiogenesis and cell migration by targeted aquaporin-1 gene disruption. Nature 434: 786-792, 2005.
22. Sanada F, Taniyama Y, Iekushi K, Azuma J, Okayama K, Kusunoki H, Koibuchi N, Doi T, Aizawa Y and Morishita R: Negative action of hepatocyte growth factor/c-Met system on angiotensin II signaling via ligand-dependent epithelial growth factor receptor degradation mechanism in vascular smooth muscle cells. Circ Res 105: 667-675, 2009.
23. Sanada F, Taniyama Y, Azuma J, Iekushi K, Dosaka N, Yokoi T, Koibuchi N, Kusunoki H, Aizawa Y and Morishita R: Hepatocyte growth factor, but not vascular endothelial growth factor, attenuates angiotensin II-induced endothelial progenitor cell senescence. Hypertension 53: 77-82, 2009.
24. Wang BW, Wu GJ, Cheng WP and Shyu KG: Mechanical stretch via transforming growth factor-β1 activates microRNA-208a to regulate hypertrophy in cultured rat cardiac myocytes. J Formos Med Assoc 112: 635-643, 2013.